



Dynamic Disturbance Effects of Proposed Tunnel Blasting on Adjacent Existing Tunnels: a Pre-Assessment Case Study

Fei Lin^{1,2}, Zhigang Zhang², Jinhua Chen², Longhao Ma^{3*}, Xiaohong Zhou²

¹ School of Resources and Safety Engineering, Chongqing University, Chongqing 400030, China

² China Coal Technology Engineering Group Huaibei Blasting Technology Research Institute Limited Company, Huaibei 235000, China

³ School of Civil Engineering, Luoyang Institute of Science and Technology, Henan 471023 Henan, China

* E-mail: mlh@cqu.edu.cn

Abstract. The construction process of the proposed tunnel will have a disruptive impact on the safe operation of adjacent subways. Therefore, taking the parallel section of the proposed Metro Line 6 and the existing Metro Line 10 in Chongqing as the research object, the geological conditions and the mechanical properties of the surrounding rocks are obtained through geological investigations and tests. Subsequently, a blasting scheme was designed for the blasting construction of the proposed tunnel, and the stress state and vibration distribution law of the existing subway lining were analyzed through simulation. Immediately afterwards, the adaptive optimal kernel spectrum method (AOK) is introduced to analyse the principal frequency characteristics of each section. The results show that the proposed underground excavation will cause additional stress on the lining structure and structure deformation, but the displacement, displacement increments and stress are within safe limits. The blast velocities in the arch and bottom of the existing tunnel are higher than those in other locations, while the arch velocity decreases with increasing distance, and the bottom velocity remains at a high level. The settlement and stress of Line 10 second lining are within the safe range.

Keywords: proposed metro, dynamic characteristics, vibration velocity, dominant frequency

1 INTRODUCTION

For the past few years, more and more metro construction projects are under construction. These projects will generally cross nearby buildings and other dense areas of pedestrian traffic. The use of the D&B method will undoubtedly cause disturbance of the surrounding buildings, which threatens the safety of nearby residents and the stability of the structure.

© The Author(s) 2024

B. Yuan et al. (eds.), *Proceedings of the 2024 8th International Conference on Civil Architecture and Structural Engineering (ICCASE 2024)*, Atlantis Highlights in Engineering 33,

https://doi.org/10.2991/978-94-6463-449-5_17

The loading-unloading wave derived from the blasting disturbance outside the tunnel is very easy to cause damage to nearby buildings [1]. Qiu et al. [2] analyzed the impact of the location of the explosion source, blast distances and burial depths on the damage form, damage evolution and stress variation patterns of existing roadways. Given the strong disturbance of the rear tunnel lining caused by the blasting load of antecedent tunnel. Zhao [3] analyzed the influence of rock properties and blasting parameters on the changing pattern of PPV in antecedent tunnel. They proposed some control measures to reduce the peak vibration velocity. Li [4] discussed the principle of the role of ground stress and blast waveforms in influencing the evolution law and distribution form of strain energy in tunnels. The research results show that for tunnel blasting under high in-situ pressure, the dynamic disturbance caused by low frequency is more likely to lead to structural damage of the tunnel. For the destructive events inside the tunnel due to external blast loads, some scholars have carried out adequate research regarding structural blast resistance and seismic design [5-6]. Among them, Mandal et al. [7] compared the response patterns of the horseshoe, circular and box-shaped tunnels under blasting loads. Further elucidated the impact of charge, lining thickness and coverage depth on the blast-bearing performance of the tunnels, ultimately identifying the most vulnerable and resistant tunnel structures under the blast damage results for different tunnel shapes. Ma et al. [8] focused on the instability of collapse and spalling of horizontal layered rock tunnel under blasting load and analyzed the blasting failure mode, damage mechanism and real-time damage evolution law of homogeneous rock and horizontally layered rock. Sadique et al. [9] examined the changes in vibration acceleration, pressure, strain energy, lining axial force, deformation, wave velocity and damage of granite, basalt and quartzite tunnels under blasting load by the finite element method. They compared the blast resistance of the three types of rock tunnels based on the above parameters.

Some scholars have also carried out some work on the blast resistance and design rationality of the tunnel structure from two perspectives, namely numerical simulation [10] and field measurements [11-12]. Among them, Goel et al. [13] studied the dynamic response of tunnels with two rock types and three-section shapes under blasting loads. They used a plastic damage model to analyse the distribution of blasting damage in different tunnels shapes. They determined that circular tunnels are the most resistant to blast loads. Qian et al. [14] analyzed the impact of explosive content on the structure of underground galleries. The results showed that measures such as shear reinforcement arrangement increased pipe wall thickness, and increased burial depth could help to strengthen the comprehensive blast resistance of the galleries.

In summary, scholars have made great efforts and achieved remarkable results in tunnel blasting damage evolution, and blasting effects. However, the research and pre-assessment of the disturbance effects of blasting on existing tunnels in close parallel sections are insufficient. This paper used the proposed Line 6 branch tunnel project in Chongqing as a background, applied surveys and tests to analyse the geological conditions and the nature of the surrounding rocks, and designed a site blasting plan. Numerical simulations were used to pre-assess the dynamic disturbance impact of the pro-

posed Line 6 tunnel excavation on the existing Line 10 in terms of stress field distribution, section maximum vibration velocity and primary frequency characteristics, respectively.

2 BACKGROUND OF THE MTR TUNNEL PROJECT

The tunnel studied in this paper is part of the Chongqing Railway Line 6 extension project, and the main section of the project is from Yuelai station to Wangjiazhuang station. The starting mileage of the tunnel in this section is K12+213 ~ K13+932.135. The tunnel section is arranged along the north-south direction and parallel to the existing Line 10 tunnel. The proposed tunnel is mainly composed of grey fine to medium-grained sandstone, primarily consisting of quartz, feldspar and a small amount of mica. The comprehensive grade of the surrounding rock is III.

3 BLASTING MODEL CALCULATION RESULTS AND ANALYSIS

3.1 Geometric and Material Models for Blasting in Metro Tunnels

The upper surface of the model is free surface, and non-reflecting limitation is applied on all sides (Fig. 1). The fierce model is not directly established when simulating the instantaneous effect of explosive blasting, but the simplified impact load is adopted. The blasting load is simplified by referring to the attenuation law of free field of air explosion proposed by Henrych in 1979 [15]. The expression of the free field of air explosion is as follows:

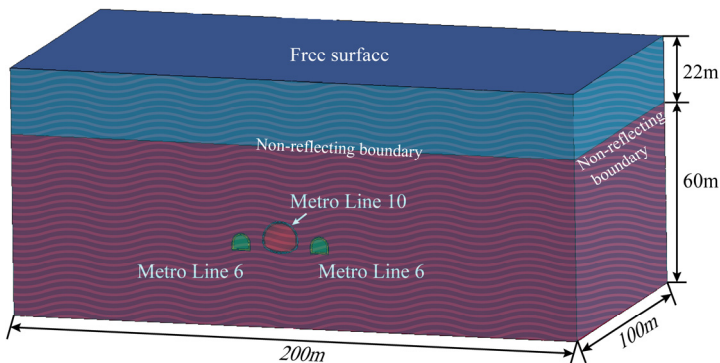


Fig. 1. Geometric model

$$\left\{ \begin{array}{l} \Delta P_{max}|_{Henrych} = \frac{14.072}{Z} + \frac{5.54}{Z^2} - \frac{0.357}{Z^3} + \frac{0.00625}{Z^4} \quad 0.05 \leq Z < 0.3 \\ \Delta P_{max}|_{Henrych} = \frac{6.194}{Z} - \frac{0.326}{Z^2} + \frac{2.132}{Z^3} \quad 0.3 \leq Z < 1 \\ \Delta P_{max}|_{Henrych} = \frac{0.662}{Z} + \frac{4.05}{Z^2} + \frac{3.288}{Z^3} \quad Z \geq 1 \end{array} \right. \quad (1)$$

Where ΔP_{max} is the peak overpressure in front of the blast incident wave. Z is the scale distance, the value of Z can be determined by the Eq. 2.

$$Z = R / Q^{1/3} \quad (2)$$

Where R is the distance. Q is the maximum charge.

Referring to the maximum charge of each section of explosives, We determined that the single section cut explosive amount of 6.63kg is used as the load peak of triangular wave [16]. According to the distance between the detonation point and the loading point of Metro Line 6 is 3.47 m. $Z=1.85$ is calculated, and according to the segmental range of Z in Eq. (1), the maximum overpressure in front of the blast incident wave is determined to be 2.06 MPa.

3.2 Blasting Vibration Characteristics of Metro Tunnels

The vertical displacement, compressive stress and tensile stress of the second lining of Line 10 are shown in Fig. 2. The second lining of the Line 10 tunnel begins to sink due to the continuous disturbance of Metro Line 6 blasting and self-weight stress, with the maximum sinking increment of 0.883mm, and the sinking point is located at the tunnel vault. The compression effect at the Secondary lining arch waist is pronounced, and the maximum compressive stress is 0.180mpa, while the tensile stress at the foot of the second lining arch is apparent, and the ultimate tensile stress is 0.169mpa. Based on the displacement and stress values of the arch bottom, the tunnel excavation of line 6 will inevitably lead to the deformation of the second lining of the Line 10 tunnel, increasing the internal force of the lining structure. However, the cumulative deformation increment, the maximum tensile, and compressive stress of Line 10 do not exceed the specified limit.

To find out the extent of blasting damage to the second lining of Line 10, we selected five sections along the axis of Line 10 (Fig. 3). Fig.4 shows the distribution law of blasting vibration combined velocity at each measuring point of 5 sections. It can be seen that the general blasting velocity distribution law of sections 3-5 is relatively consistent, showing that the vibration velocity values of the left arch and arch bottom are greater than those at other locations. With the increase of the distance, the blasting vibration velocity distribution of section 1 and section 2 shows a trend of increasing the arch bottom and decreasing at other locations.

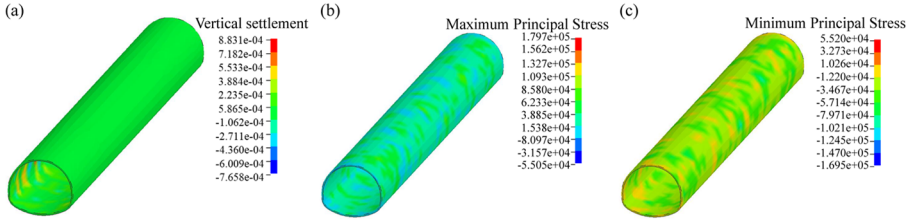


Fig. 2. Metro Line 10 displacement and stress field clouds

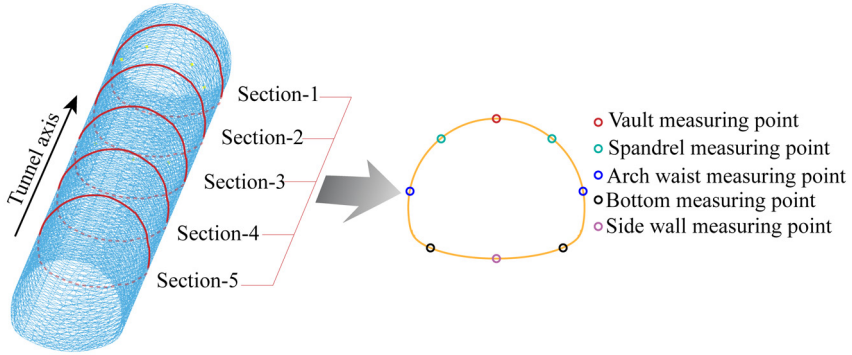


Fig. 3. Layout of blasting vibration measuring points

In summary, the effect of blast distance on the distribution of vibration velocity is significant, and this is mainly reflected in the following characteristics: 1) The vibration velocity of arch bottom and local area of arch is greater than that of other positions under close distance. 2) In the long distance conditions, the arch vibration velocity rapidly reduced, while the bottom of the arch vibration velocity value is still in a high position. Overall, the blasting vibration velocity of each section is below the control value of 2 cm/s, which does not damage the lining structure of the existing Line 10 tunnel.

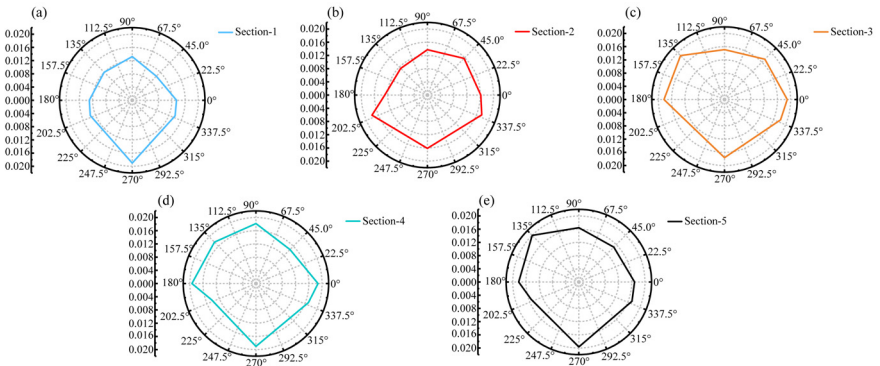


Fig. 4. Velocity distribution of measuring points on each section

3.3 Dominant Frequency Characteristics

The blast vibration signal spectra of Section 1 were plotted by combining AOK theory and MATLAB programming, as shown in Fig. 5. There are many blasting vibration frequency components at the vault of section 1, the main frequency range of vault is between 0 and 40 Hz, the frequency component range of arch shoulder is between 0 and 20 Hz, the main frequency of arch waist is between 0 and 15Hz, and the main frequencies at side wall and arch bottom are lower than 10 Hz. Referring to blasting safety regulations, the self-vibration frequency of the structure is generally between 2 and 5 Hz, which indicates that there is the possibility of resonance at local positions of line 10 under the influence of blasting vibration of line 6. Therefore, the blasting design scheme for Line 6 still needs to be improved, particularly in controlling the amount of charge in each section of the shell hole. In response to the above, we recommend the following measures for construction sites: Micro-differential and weak blasting, over-support and over-pre-reinforcement, or a ring of damping holes should be added to the periphery of the perimeter holes.

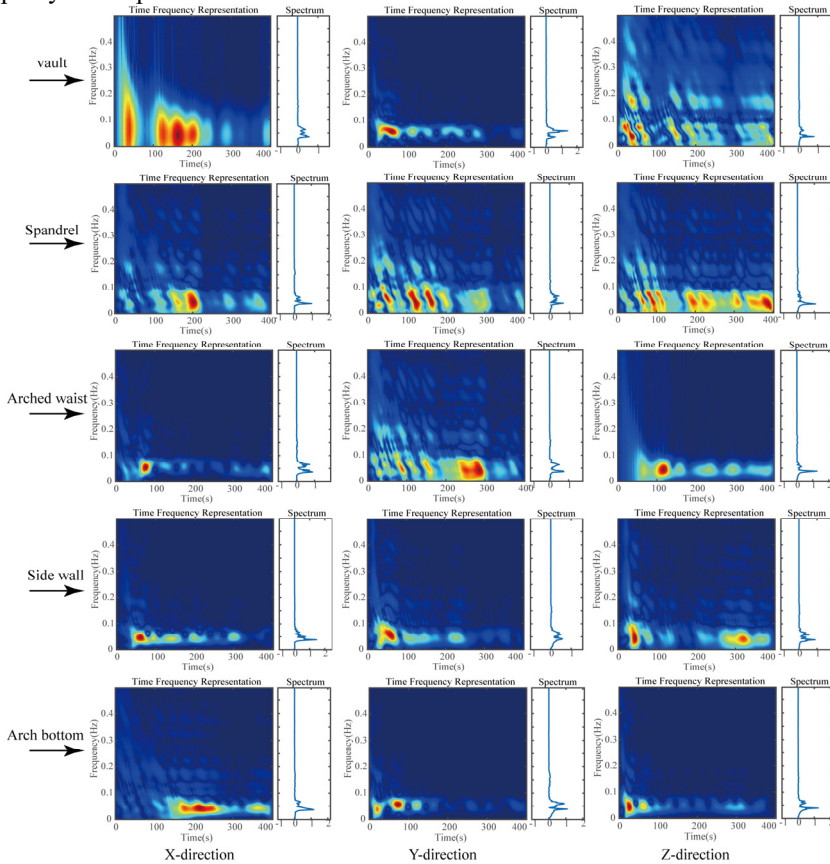


Fig. 5. Time frequency diagram of vibration signal for segment-1

4 CONCLUSIONS

(1) Through site investigation and indoor tests, it was determined that the perimeter rock at the site is Grade III. The nature of the perimeter rock is mainly sandstone.

(2) Each section shows that the combined blast vibration velocity is most significant at the left arch and the arch bottom. As the blast distance increases, the combined velocity value at the bottom remains high, while the combined velocity at the arch gradually decreases.

(3) Based on the adaptive optimal kernel principle, the central frequency distribution of the existing Line 10 tunnel was obtained by MATLAB programming. The frequency range of the vault position was 0~40Hz, and the main frequency of other places was mainly concentrated in 0~10 Hz. This situation shows that the vibration frequency of the existing Line 10 is at a low frequency. Still, the self-vibration frequency of the tunnel lining structure is generally between 2~5 Hz, so there is a possibility that blasting vibration of the proposed Line 6 tunnel may cause resonance of the existing Line 10 lining structure. To ensure the normal operation of Line 10, it is recommended to reasonably control the maximum single section charge and the detonation interval between each sections at the tunnel blasting site. Meanwhile, the support measures for the arch should be strengthened, such as over-strengthening and over-supporting and a ring of damping holes can also be set around the periphery of the tunnel arch to reduce the blasting disturbance.

ACKNOWLEDGMENTS

This study was supported by the Research on Intelligent Prediction Technology of Blasting vibration of open-pit mine (2022-2-TD-QN006).

DATA AVAILABILITY STATEMENT

The datasets of the study are available on request from the authors.

CONFLICTS OF INTERESTS

The authors(s) declared no potential conflicts of interest with respect to the research, authorship, and/or publication of this article.

REFERENCES

1. Wu PF, Yang TJ and Jia WC. Reliability Analysis and Prediction on Tunnel Roof under Blasting Disturbance. *KSCE J. Civ. Eng.* **2019**, *23*, 4036-4046.
2. Qiu J, Li D, Li X, et al. Numerical investigation on the stress evolution and failure behavior for deep roadway under blasting disturbance. *Soil Dyn. Earthq.* **2020**, *137*, 1-13.

3. Zhao X, Sun K, Xu W, et al. Safety Analysis of Lining Structure Influenced by Blasting of Tunnel with Extralarge Section and Small Space. *Shock Vib.* **2020**, *2020*, 1-14.
4. Li C and Li X. Influence of wavelength-to-tunnel-diameter ratio on dynamic response of underground tunnels subjected to blasting loads. *Int. J. Rock Mech. Min. Sci.* **2018**, *112*, 323-338.
5. Song S, Li S, Li L, et al. Model test study on vibration blasting of large cross-section tunnel with small clearance in horizontal stratified surrounding rock. *Tunn. Undergr. Space Technol.* **2019**, *92*, 1-7.
6. Huang J, Luo Y, Zhang G, et al. Numerical analysis on rock blasting damage in Xiluodu underground powerhouse using an improved constitutive model. *Eur. J. Environ. Civ. Eng.* **2020**, *26*, 3009-3026.
7. Mandal J, Agarwal AK and Goel MD. Numerical Modeling of Shallow Buried Tunnel Subject to Surface Blast Loading. *J. Perform. Constr. Facil.* **2020**, *34*, 1-11.
8. Ma LH, Jiang X, Chen J, et al. Analysis of Damages in Layered Surrounding Rocks Induced by Blasting During Tunnel Construction. *Int. J. Struct. Stab. Dyn.* **2021**, *21*, 1-27.
9. Sadique MR, Zaid M and Alam MM. Rock Tunnel Performance Under Blast Loading Through Finite Element Analysis. *Geotech. Geol. Eng.* **2021**, *40*, 35-56.
10. Ma LH, Lin F, Liu R, et al. Disturbance and control of national strategic gas storage induced by adjacent tunnel blasting. *Front. Earth Sci.* **2022**, *9*, 1-12.
11. Lin F, Liu R, Zhang ZG, et al. Reduction of blasting induced ground vibrations using high-precision digital electronic detonators. *Front. Earth Sci.* **2022**, *9*, 1-9.
12. Ma LH, Chen J, Zhao YF, et al. Water content and bedding angle effects on the mechanical properties and Micro-/Macro-failure mechanism of phyllite. *Arab. J. Sci. Eng.* **2022**, 1-19.
13. Goel MD, Verma S and Panchal S. Effect of Internal Blast on Tunnel Lining and Surrounding Soil. *Indian Geotech. J.* **2021**, *51*, 359-368.
14. Qian H, Zong Z, Wu C, et al. Numerical study on the behavior of utility tunnel subjected to ground surface explosion. *Thin-Walled Struct.* **2021**, *161*, 1-18.
15. Dadkhah H and Mohebbi M. Performance assessment of an earthquake-based optimally designed fluid viscous damper under blast loading. *Adv. Struct. Eng.* **2019**, *22*, 3011-3025.
16. Li X and Weng L. Numerical investigation on fracturing behaviors of deep-buried opening under dynamic disturbance. *Tunn. Undergr. Space Technol.* **2016**, *54*, 61-72.

Open Access This chapter is licensed under the terms of the Creative Commons Attribution-NonCommercial 4.0 International License (<http://creativecommons.org/licenses/by-nc/4.0/>), which permits any noncommercial use, sharing, adaptation, distribution and reproduction in any medium or format, as long as you give appropriate credit to the original author(s) and the source, provide a link to the Creative Commons license and indicate if changes were made.

The images or other third party material in this chapter are included in the chapter's Creative Commons license, unless indicated otherwise in a credit line to the material. If material is not included in the chapter's Creative Commons license and your intended use is not permitted by statutory regulation or exceeds the permitted use, you will need to obtain permission directly from the copyright holder.

